

+ 3.9 + 1.3 - 1.8 + 1.1 = 33.1 cm³ mol⁻¹. The term $[\Delta V_{\text{elong}}^{\circ}(\text{Ni}(\text{hedta})^{-}) - \Delta V_{\text{elong}}^{\circ}(\text{Ni}(\text{edda}))]$ should be added as a correction term for the electron donation from the third carboxylate coordinated in Ni(hedta)⁻. The electrostriction for this case may be considered by the following reaction, in which we have one uninegative anion on both sides: Ni(edda) + OAc⁻ ⇌ Ni(edda)(OAc)⁻. Therefore we neglected the contribution of electrostriction, which may be regarded as small.

From $\Delta V^{\circ}(\text{Ni}(\text{edda}))$ we calculated $\Delta V^{\circ}(\text{Ni}(\text{edta})^{2-})$ as follows: $\Delta V^{\circ}(\text{Ni}(\text{edta})^{2-}) = \Delta V^{\circ}(\text{Ni}(\text{edda})) + 2\Delta\Delta V^{\circ}(\text{Ni}(\text{gly})^{+}) - 2\Delta\Delta V^{\circ}(\text{Ni}(\text{NH}_3)^{2+}) - \Delta V_{\text{elong}}^{\circ}(\text{Ni}(\text{edda})) + \Delta V_{\text{elong}}^{\circ}(\text{Ni}(\text{edta})^{2-}) + \Delta V_{\text{elec}}^{\circ}(\text{Ni}(\text{edda})(\text{OAc})_2^{2-}) = 28.6 + 7.8 + 2.6 - 1.8 + 0 + 3.2 = 40.4 \text{ cm}^3 \text{ mol}^{-1}$. We took into account the contribution of electrostriction from the following reaction (the last term): Ni(edda) + 2OAc⁻ ⇌ Ni(edda)(OAc)₂²⁻.

Yoshitani has recently reported 33.7 and 44.4 cm³ mol⁻¹ as reaction volumes for the formation of Ni(hedta)⁻ and Ni(edta)²⁻, respectively.²⁷ The calculated reaction volumes for the formation

of Ni(edda) and Ni(hedta)⁻ compare very favorably with the experimental values. The experimental value for Ni(edta)²⁻ is a little too high as compared with the calculated value.

In conclusion the following four factors are important in the consideration of the reaction volume for the formation of metal complexes: electrostriction, contraction of donor atoms in the first coordination sphere, expansion of metal complexes by the elongation of the bond M-OH₂ due to bound amine(s) and/or carboxylate(s), and the volume chelate effect.

Acknowledgment. This research has been supported by a Grant-in-Aid for Scientific Research (Grant No. 62470041) and a Grant-in-Aid for Special Project Research (Grant No. 62124039) from the Ministry of Education, Science, and Culture of Japan.

Registry No. HOAc, 64-19-7; en, 107-15-3; Hgly, 56-40-6; Hsar, 107-97-1; H₂edda, 5657-17-0.

Supplementary Material Available: Plots of \bar{q}_H against $-\log [H^+]$ (Figure s1), plots of \bar{n}_L vs $-\log [L]$ (Figure s2), compositions of solutions used for the Ni(II)-glycine system (Table sI), and moles of species in reactions occurring by mixing in the Ni(II)-glycine system (Table sII) (9 pages). Ordering information is given on any current masthead page.

(27) Yoshitani, K. *Bull. Chem. Soc. Jpn.* **1985**, *58*, 1646.

(28) See paragraph at end of paper regarding supplementary material.

Contribution from the Departamento de Química Inorgánica, Facultad de Ciencias, Universidad de Málaga, Apartado 59, 29071 Málaga, Spain

Synthesis and Characterization of Mixed Niobium-Vanadium Phosphates

A. L. García-Ponce, L. Moreno-Real, and A. Jiménez-López*

Received January 13, 1988

From solutions containing several percentage molar ratios V/(V + Nb), mixed niobyl-vanadyl phosphates were obtained. The mixed phosphate with maximum vanadium content was 21%. From analysis by EDX-SEM, DTA, IR spectra, X-ray diffraction, and diffuse-reflectance spectra, it was established that the mixed phosphates are solid solutions.

Introduction

Compounds with the formula MOAO₄ (M = V, Nb, Ta; A = P, As) constitute an isomorphic series that has two types of crystal forms: one tetragonal and the other orthorhombic. X-ray diffraction studies have established the structure of tetragonal forms MOPO₄¹⁻³ and MOAsO₄^{4,5} which consist of chains of corner-shared [MO₆] octahedra running parallel to the *c* axis. In the *ab* plane, each [MO₆] octahedron shares corners with four [AO₄] tetrahedra, which link the octahedral chains to produce a three-dimensional lattice. The layers of these compounds along the *c* axis are linked by the trans oxygen vertices of the octahedra. However, the M atoms are not centered within the octahedra but displaced along the *c* axis so that it can establish two M-O linkages; one is short, which corresponds to a M=O bond; the other is longer, a simple M-O linkage and therefore weaker.

Hydrates of some of these compounds are known, and their formation may be explained by breaking of the long M-O linkages of the respective anhydrous forms and subsequent substitution of the O of the adjacent layer by a water molecule in the sixth coordination position of the metal. Hydrates of this kind are reported for VOPO₄,^{6,7} VOAsO₄,⁴ NbOPO₄,⁸ and NbOAsO₄,⁵ which have a variable number of water molecules and present a tetragonal structure similar to that of their respective anhydrous forms.

It is interesting that this type of compound may undergo intercalation reactions in which the matrix of the original product is preserved throughout. Two types of intercalation reactions have been described: (1) those in which alcohols,^{9,10} amines,^{10,11} or amides¹² enter the interlamellar space to coordinate with the metal atom, either by direct means or through a water molecule, and

(2) those in which the laminar charge produced by the reaction of vanadium(V) to vanadium(IV) is compensated by the intercalation of inorganic¹³ or organic¹⁴ cations.

However, vanadyl phosphates and arsenates have a poor hydrolytic stability, which leads to the solid being partially dissolved^{13,14} especially during redox intercalation reactions in aqueous media. To circumvent this, solvents like acetone¹⁴ or aqueous alcoholic mixtures¹³ are used. On the other hand, although aqueous suspensions of the niobyl phosphates and arsenates have great stability, they have an important limitation because niobium itself is highly stable in the (V) oxidation state and cannot undergo the type of redox topotactic intercalation reactions induced by moderate reducing agents.

- (1) Jordan, B.; Calvo, C. *Can. J. Chem.* **1973**, *51*, 2621-2625.
- (2) Longo, J. M.; Kierkegaard, P. *Acta Chem. Scand.* **1966**, *20*, 72-78.
- (3) Longo, J. M.; Pierce, J. W.; Kafalas, J. A. *Mater. Res. Bull.* **1971**, *6*, 1157-1166.
- (4) Chernorukov, N. G.; Egorov, N. P.; Korshunov, I. A. *Zh. Neorg. Khim.* **1978**, *23*, 2672-2675; *Russ. J. Inorg. Chem. (Engl. Transl.)* **1978**, *23*, 1479-1481.
- (5) Chernorukov, N. G.; Egorov, N. P.; Korshunov, I. A. *Izv. Akad. Nauk SSSR, Neorg. Mater.* **1979**, *15*, 335-338.
- (6) Bordes, E.; Courtine, P.; Pannetier, G. *Ann. Chim. (Paris)* **1973**, *8*, 105-113.
- (7) Ladwig, G. Z. *Anorg. Allg. Chem.* **1965**, *338*, 266-278.
- (8) Chernorukov, N. G.; Egorov, N. P.; Mochalova, I. R. *Zh. Neorg. Khim.* **1978**, *23*, 2931-2934; *Russ. J. Inorg. Chem. (Engl. Transl.)* **1978**, *23*, 1627-1629.
- (9) Benes, L.; Votinsky, J.; Kalousova, J.; Klikorka, J. *Inorg. Chim. Acta* **1986**, *114*, 47-50.
- (10) Beneke, K.; Lagaiy, G. *Inorg. Chem.* **1983**, *22*, 1503-1507.
- (11) Johnson, J. W.; Jacobson, A. J.; Brody, J. F.; Rich, S. *Inorg. Chem.* **1982**, *21*, 3820-3825.
- (12) Martínez-Lara, M.; Moreno-Real, L.; Jiménez-López, A.; Bruque-Gómez, S. *Rodriguez-García, A. Mater. Res. Bull.* **1986**, *21*, 13-22.
- (13) Jacobson, A. J.; Johnson, J. W.; Brody, J. F.; Scanlon, J. C.; Lewandowski, J. T. *Inorg. Chem.* **1985**, *24*, 1782-1787.
- (14) Martínez-Lara, M.; Jiménez López, A.; Moreno-Real, L.; Bruque, S.; Casal, B.; Ruiz-Hitzky, E. *Mater. Res. Bull.* **1985**, *20*, 549-555.

* To whom correspondence should be addressed.

This present work describes the synthesis of mixed niobyl–vanadyl phosphate hydrates designed to confer the following two important characteristics of the precursors to the mixed compound: first, the capacity to undergo topotactic redox reactions of $\text{VOPO}_4 \cdot 2\text{H}_2\text{O}$ ^{13,14} and, second, the high thermal and hydrolytic stability of $\text{NbOPO}_4 \cdot 3\text{H}_2\text{O}$.⁸ Furthermore, the characterization of these synthetic mixed phosphates would lead to the identification of the modifications produced by the introduction of the vanadium into the niobyl phosphate framework.

Experimental Section

Preparation of the Niobyl–Vanadyl Phosphates. The preparation of the mixed niobyl–vanadyl phosphates in every case started with one of a series of 20-g mixtures of Nb_2O_5 and V_2O_5 , each with a different $100[\text{V}/(\text{Nb} + \text{V})]$ percentage molar ratio as follows: 5, 10, 15, 20, 25, 30, and 40%. Each mixture was dissolved by adding 145 mL of hydrofluoric acid (45% w/w), followed by 15 mL of nitric acid (60% w/w). Then 90 mL of phosphoric acid (85% w/w) was added, and the resulting solution was heated in a water bath until a crystalline yellow compound precipitated. After the solid was separated, it was resuspended in 5 M nitric acid solution to provide an oxidizing medium to stabilize the vanadium in the (V) oxidation state. In the precipitation process of the mixed niobyl–vanadyl phosphates, vanadyl phosphate coprecipitated and was eliminated by successive washings with water and centrifugation. The products were air-dried and stored in vessels kept at 76% relative humidity; this was provided by a saturated solution of sodium chloride.

The methods employed for the synthesis of $\text{NbOPO}_4 \cdot 3\text{H}_2\text{O}$ and $\text{VOPO}_4 \cdot 2\text{H}_2\text{O}$ were described in previous publications.^{14,15}

Characterization of the Products. The chemical composition of the products was determined by dissolution of the solid in hydrofluoric acid and joint precipitation of cupferron complexes of niobium and vanadium. These complexes were calcined to oxides at 1000 °C. Vanadium was analyzed by potentiometric measurements with a ferrous salt. Phosphorus was determined by colorimetric analysis as the blue molybdo-phosphate complex. The water was calculated from gravimetric measurements after calcination to 500 °C to obtain the phosphates in their anhydride form.

The hydrolytic stability of these mixed phosphates and the vanadyl phosphate was studied in aqueous suspensions under two different conditions: 0.2 g of the samples was added to (1) 20 mL of water at 50 °C for 90 h and (2) 20 mL of a CsI solution of the adequate concentration to yield the ratio $\Gamma/\text{V}^{5+} = 5$ at 25 °C for 70 h. After centrifugation the phosphate content in the supernatants was determined.

Both the scanning electron microscope studies (SEM) and the X-ray fluorescence studies (EDX) were carried out with a JEOL Temscan 100 EC microscope equipped with a microprobe using Kevex S 100 C energy dispersion. The samples were prepared from ultrasonicated aqueous suspensions of the solids. Drops of these were placed on a copper grid and covered with gold.

X-ray diffraction (XRD) studies were carried out on both the orientated aggregates and the powder diffractograms of the samples with a Siemens D501 automated diffractometer using graphite-monochromated $\text{Cu K}\alpha$ radiation.

Thermal analyses (TGA and DTA) were carried out on a Rigaku Thermoflex instrument. The samples were heated in air at a rate of 10 $\text{K}\cdot\text{min}^{-1}$ with calcined Al_2O_3 as the reference standard. Platinum crucibles were used, and the thermocouples consisted of Pt/Pt–Rh. Infrared spectra were recorded on a Beckman 4260 spectrometer with a spectral range of 4000–200 cm^{-1} , using dry KBr pellets containing 2% of the product. The diffuse-reflectance spectra (UV–vis) were obtained on a Kontron Uvikon 810 spectrophotometer using pressed tablets of BaSO_4 as the reference.

Results and Discussion

The vanadyl phosphate coprecipitated during the synthesis of these mixed phosphates was eliminated by successive washings with water because its aqueous solubility is conveniently much greater than that of the mixed phosphates, permitting a clear separation. The X-ray diffraction studies of the orientated aggregates in high hydration states serve as a control to confirm the complete elimination of the coprecipitated vanadyl phosphate in the wash phase. Its presence in even very low amounts shows as a sharp reflection at 10.5 Å, which corresponds to the basal spacing of $\text{VOPO}_4 \cdot 5\text{H}_2\text{O}$,¹⁰ while the reflections of the mixed niobyl–vanadyl phosphates presented an appearance similar to that of

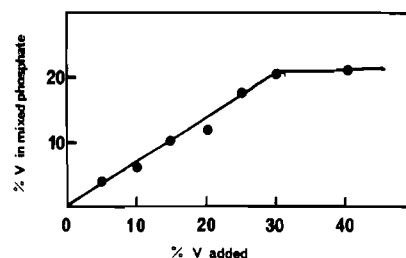


Figure 1. Variation of vanadium incorporated in the mixed phosphate as a function of vanadium added expressed in percentage molar ratios.

Table I. Analytical Data for $(\text{V}_x\text{Nb}_{1-x})\text{OPO}_4 \cdot n\text{H}_2\text{O}^a$

% V_i	% V_s	stoichiometric formula
5	4.0	$(\text{V}_{0.04}\text{Nb}_{0.96})\text{OPO}_4 \cdot 2.7\text{H}_2\text{O}$
10	5.8	$(\text{V}_{0.06}\text{Nb}_{0.94})\text{OPO}_4 \cdot 2.7\text{H}_2\text{O}$
15	10.3	$(\text{V}_{0.10}\text{Nb}_{0.90})\text{OPO}_4 \cdot 2.8\text{H}_2\text{O}$
20	11.4	$(\text{V}_{0.11}\text{Nb}_{0.89})\text{OPO}_4 \cdot 2.8\text{H}_2\text{O}$
25	17.4	$(\text{V}_{0.17}\text{Nb}_{0.83})\text{OPO}_4 \cdot 2.6\text{H}_2\text{O}$
30	20.6	$(\text{V}_{0.21}\text{Nb}_{0.79})\text{OPO}_4 \cdot 2.8\text{H}_2\text{O}$
40	21.1	$(\text{V}_{0.21}\text{Nb}_{0.79})\text{OPO}_4 \cdot 2.7\text{H}_2\text{O}$

^a Values are given as percentages in moles of V in comparison with moles of Nb + V (a) in the reaction mixture (V_i) and (b) in the synthesized solid (V_s).

niobyl phosphate, a basal spacing of between 7.9 and 8.0 Å for the same hydration conditions.

The formation of the mixed phosphates may be considered to be a gradual process of isomorphic substitution of the niobium of the niobyl phosphate structure by vanadium, which is incorporated into the original matrix. This substitution is facilitated because the introduced vanadium has a smaller radius than the niobium it replaces and so does not produce great distortion in the mixed-phosphate crystal lattice. The experimental synthetic process employed an increasing series of $\text{V}/(\text{Nb} + \text{V})$ percentage molar ratios to define the degree of replacement of niobium by vanadium in each case and also the maximum substitution possible for the lattice framework.

Figure 1 shows that the vanadium content of the mixed phosphates (V_s) increased proportionately to vanadium added (V_i) until the amount introduced into the framework reached the level of 20%. When the percentage level of vanadium in the synthesis process was increased, further incorporation was considerably decreased so that the graph shows a plateau that tends toward a value of 21%, the maximum vanadium content of the network. Although, in general, vanadium content increased directly with the percentage of vanadium in the solutions, its relative level of inclusion, expressed as $100(\text{V}_s/\text{V}_i)$, decreased from 81% to 53% in a progression from the lowest to the highest vanadium contents of the mixed phosphates.

Table I shows the percentages of vanadium used in the synthesis and also the percentages found in the solid, together with the stoichiometric formulas of the synthetic mixed niobyl–vanadyl phosphates, which were calculated from their chemical analysis. The number of molecules of water per formula unit varied considerably according to the relative humidity conditions to which the sample had been exposed: for a humidity of 76% this number ranged from 2.6 to 2.8.

In the SEM photomicrograph of the mixed phosphate with the highest vanadium content, $(\text{V}_{0.21}\text{Nb}_{0.79})\text{OPO}_4 \cdot 2.7\text{H}_2\text{O}$ (Figure 2), crystalline aggregates were observed with different particle sizes. In the center of the aggregates there was a well-defined pile of particles that confirmed the laminar nature of these mixed compounds. On the other hand, in all directions from the center of the sample microcrystals appeared to have a uniform habit. To check the homogeneity of the microcrystal composition, an analysis by electronic microprobe was carried out. Several crystalline aggregates were explored, and this exploration included several different points in the same crystal. The intensities of the characteristic emissions Nb $L\alpha$ and V $K\alpha$ (Table II) were acceptably constant for the different crystals and for separate points

(15) Bruque, S.; Martínez-Lara, M.; Moreno-Real, L.; Jiménez-López, A.; Ruiz-Hitzky, E.; Sanz, J. *Inorg. Chem.* **1987**, *26*, 847–850.

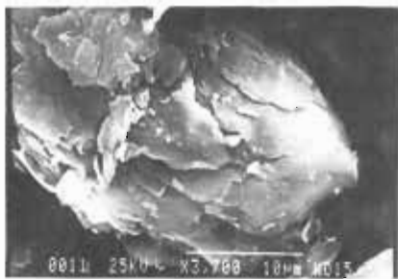


Figure 2. SEM photomicrograph of $(V_{0.21}Nb_{0.79})OPO_4 \cdot 2.7H_2O$. The bar in the lower right corresponds to 10 μm .

Table II. EDX Data for $(V_{0.21}Nb_{0.79})OPO_4 \cdot 2.7H_2O^a$

random particles		one crystalline aggregate only	
Nb	V	Nb	V
12.3	2.9	11.5	3.6
11.9	2.7	12.4	2.8
13.9	2.5	10.7	3.2
12.6	2.9	10.9	3.5
12.1	3.5	10.5	3.6

^a Peak areas are measured in the emissions Nb $L\alpha$ and V $K\beta$.

in the same crystal. This suggests that the sample was composed of only one type of crystal and that these crystals present a homogeneous composition.

The hydrolysis study of aqueous suspensions of the mixed phosphates indicated that temperature increases affected the hydrolytic stability more than when they were subjected to reactions in which the vanadium(V) of the framework changed to vanadium(IV) under the influence of a moderate reductant like I^- . The observed degree of hydrolysis of these mixed compounds depended on the vanadium content. The degree of hydrolysis of the mixed phosphate with the lowest content of vanadium, at 50 $^\circ C$, was 1.3%, while for the compound richest in vanadium, it reached 4.0%. However, when hydrolysis was measured after reduction with CsI at 25 $^\circ C$, the values ranged between 0.2 and 1.0%, respectively.

All the powder diffractograms of the synthesized mixed phosphates showed profiles very similar to that of niobyl phosphate. Figure 3 shows, for comparison, the principal reflections of both hydrated niobyl phosphate and the mixed niobyl–vanadyl phosphate with maximum vanadium content; both layered compounds showed basal spacings close to 8 \AA for samples equilibrated at 76% relative humidity.

In the case of the mixed phosphates, the greatest peak width corresponded to the (002) spacing, and its splitting when the relative humidity is reduced indicates that the water content in the compound has a great influence and that changes in this content provoke a variety of basal spacing values, which correspond to different hydrated phases; a similar behavior is observed for $NbOPO_4 \cdot 3H_2O$.^{10,15}

The X-ray data of all the mixed niobyl–vanadyl phosphates were indexed in the tetragonal system and gave values for the parameters of the cell unit that ranged from 6.42 to 6.45 \AA for $a = b$ and between 15.76 and 15.98 \AA for c , although the corresponding basal spacings are half the value of the c parameter (7.88–7.99). The latter fact can be explained if it is assumed that phosphate layers have a distribution sequence along the c axis in which alternate layers are displaced relative to the similar layers in the ab plane as has been described for similar systems such as layered silicates¹⁶ and phosphates.¹⁷ In any case, the interlaminar spacings, as well as the $a = b$ parameters mentioned above, are similar to those found for $NbOPO_4 \cdot 3H_2O$.⁸ It must be emphasized that no significant correlative variations of parameter a were found

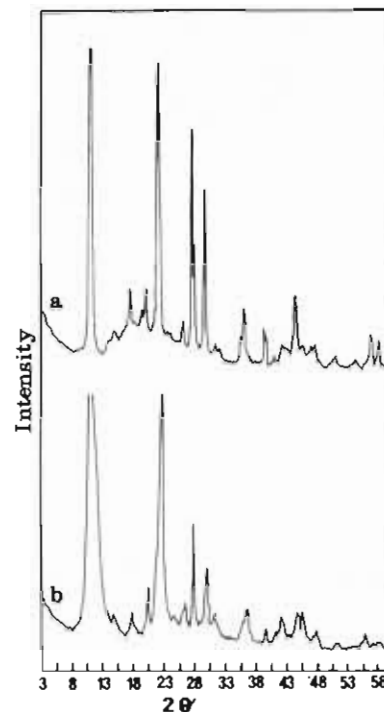


Figure 3. X-ray powder patterns of (a) $NbOPO_4 \cdot 3H_2O$ and (b) $(V_{0.21}Nb_{0.79})OPO_4 \cdot 2.7H_2O$.

Table III. X-ray Powder Diffraction Data for $(V_{0.21}Nb_{0.79})OPO_4 \cdot 2.7H_2O^a$

hkl	$d_{\text{obs.}} \text{\AA}$	$d_{\text{calc.}} \text{\AA}$	I/I_0
002	7.901	7.910	100
011	5.956	5.936	7
012	4.987	4.993	9
111	4.370	4.375	14
013	4.075	4.079	11
004	3.950	3.953	33
014	3.366	3.383	8
020	3.715	3.214	25
114	2.982	2.980	15
121	2.829	2.849	7
024	2.494	2.491	6
220	2.274	2.273	7
222	2.185	2.178	6
030	2.144	2.137	7
131	2.017	2.018	10
132	1.969	1.975	8
133	1.897	1.894	6
040	1.608	1.608	5
042	1.575	1.575	4
331	1.509	1.511	4
242	1.415	1.414	4
440	1.137	1.137	3

^a Tetragonal; $a = b = 6.431 \text{\AA}$, $c = 15.802 \text{\AA}$, $\lambda = 1.5406 \text{\AA}$.

in spite of the different composition of the synthesized series; this could be explained by the fact that the substitution of niobium by vanadium produces an almost negligible distortion in the niobyl phosphate framework. Table III shows the indexing for the reflections of mixed phosphate with the highest content of V, i.e. $(V_{0.21}Nb_{0.79})OPO_4 \cdot 2.7H_2O$.

DTA curves may serve to establish if a mixed system is a mixture of phases or a solid solution.¹⁸ When a system is formed by two or more phases, the thermal behavior of each phase is independent of the other; the resultant thermogram is then the sum of the effects of each component. Figure 4 shows the DTA diagrams for $NbOPO_4 \cdot 3H_2O$ and $VOPO_4 \cdot 2H_2O$. The trihydrated niobyl phosphate showed three endothermic effects at 40, 70, and

(16) Walker, G. W. In *Inorganic Components*; Gieseking, J. E., Ed.; Soil Components 2; Springer-Verlag: New York, 1975.
 (17) Clearfield, A. In *Inorganic Ion Exchange Materials*; Clearfield, A., Ed.; CRC: Boca Raton, FL, 1982.

(18) Galli, P.; La Ginestra, A.; Berardelli, M. L.; Massucci, M. A.; Patrono, P. *Thermochim. Acta* **1985**, *92*, 615–618.

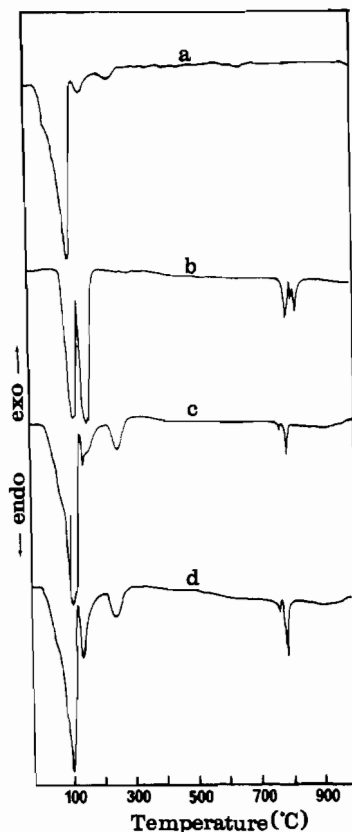


Figure 4. Thermal analysis (DTA) of (a) $\text{NbOPO}_4 \cdot 3\text{H}_2\text{O}$, (b) $\text{VOP-O}_4 \cdot 2\text{H}_2\text{O}$, and (c and d) vanadium phosphate and niobium phosphate mixtures with 11% and 21% V, respectively.

95 °C, which correspond to the loss of 1.8 mol of water/mol of phosphate. The compound has a monohydrate composition at 120 °C, and the water molecule is directly coordinated to the niobium and is eliminated at temperatures above 120 °C. This elimination occurs in distinct stages: it occurs with the first endothermic effect at 140 °C and when the last coordinated molecules are eliminated with another endothermic effect centered at 235 °C. The thermograph of $\text{VOPO}_4 \cdot 2\text{H}_2\text{O}$ is analogous; it loses one molecule of water in the first stage with an endothermic effect at 105 °C, whereas the monohydrate phase loses its last molecule of vanadium-coordinated water in one endothermic effect centered at 145 °C,⁸ unlike niobyl phosphate, whose water molecule was eliminated in several stages. This variation of behavior could be due to kinetic factors or to the fact that in the vanadyl phosphate the water molecule is more weakly coordinated to the vanadium atom. Lastly, two endothermic peaks appeared at 760 and 785 °C; they were accompanied by a slight weight loss, attributed to the loss of oxygen and the consequent reduction of the vanadium.¹⁹

The DTA curves of the mixed phosphates with low vanadium content gave profiles very similar to that of the niobyl phosphate hydrate (Figure 5). Consequently, the three first effects, which correspond to the loss of 1.6–1.8 water molecules, are still seen, although the first can be seen to decrease as one advances through the series. The loss of water coordinated to the metal (niobium or vanadium) appears to take place in closer steps in comparison with the process in $\text{NbOPO}_4 \cdot 3\text{H}_2\text{O}$. The other two overlapping endothermic effects now appear in the interval of temperature between 120 and 240 °C. The first effect appeared at a slightly higher temperature and with intensity decreased from that before, while, as the matrix vanadium content increased, the second appeared at a lower temperature. Consequently, in those compounds with 21% substitution only one endothermic effect appeared, at an intermediate temperature close to 200 °C. Furthermore, in every case, the mixed compounds showed between 2.6 and 2.8 mol of water/mol of phosphate, a content which

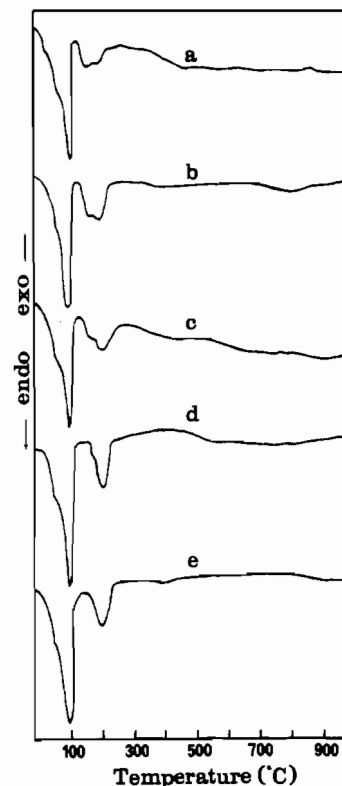


Figure 5. Thermal analysis (DTA) of (a) $(\text{V}_{0.04}\text{Nb}_{0.96})\text{OPO}_4 \cdot 2.7\text{H}_2\text{O}$, (b) $(\text{V}_{0.06}\text{Nb}_{0.94})\text{OPO}_4 \cdot 2.7\text{H}_2\text{O}$, (c) $(\text{V}_{0.11}\text{Nb}_{0.89})\text{OPO}_4 \cdot 2.8\text{H}_2\text{O}$, (d) $(\text{V}_{0.17}\text{Nb}_{0.83})\text{OPO}_4 \cdot 2.6\text{H}_2\text{O}$, and (e) $(\text{V}_{0.21}\text{Nb}_{0.79})\text{OPO}_4 \cdot 2.8\text{H}_2\text{O}$.

approximates that of niobyl “trihydrate”. It should be emphasized that the endothermic effects that appear in $\text{VOPO}_4 \cdot 2\text{H}_2\text{O}$ around 800 °C are not seen in the thermographs of the synthesized mixed compounds. This indicates that the crystalline lattice of the mixed phosphate has a high thermal stability. These results indicate that the synthesized mixed phosphates are solid solutions since their thermographs are very different from those which are given by mixtures of phases as shown by the thermograms in Figure 4.

The infrared spectra of the mixed phosphates present a profile very similar to that described for pure niobyl phosphate. Figure 6 shows the spectra for these compounds between 300 and 1800 cm^{-1} . Niobyl phosphate, in addition to showing water deformation bands at 1615 cm^{-1} , shows asymmetrical tension vibrations that arise from the splitting of the ν_3 tension band of the phosphate tetrahedra.⁸ The band at 1010 cm^{-1} overlaps with another at 995 cm^{-1} assigned to the $\text{Nb}=\text{O}$ vibrational stretching. This assignment was confirmed by the infrared spectra of a mixed niobyl–vanadyl arsenate with a low vanadium content, which showed the band corresponding to $\text{Nb}=\text{O}$ stretching clearly separated from the tension bands of the arsenate group, which appeared at lower frequencies. The stretching vibrations of the deformed octahedra [NbO_6] may also be seen at 686, 665, and 650 cm^{-1} and the O–P–O deformation modes at 400 and 380 cm^{-1} .²⁰

The mixed phosphates showed the same absorptions at the same wavenumbers as before, with the exception of that appearing at 1145 cm^{-1} , whose intensity diminished as the vanadium content of the phosphate increased while, simultaneously, there appeared a band with increasing intensity at 1100 cm^{-1} . This band is also found with high intensity in the vanadyl phosphate infrared spectra²⁰ and is assigned to $\nu_2(\text{O}-\text{P}-\text{O})$. This observation appears to indicate that the incorporation of the vanadium in the framework produces an asymmetric distortion that intensifies the observed absorption.

The diffuse-reflectance spectra of the synthesized mixed niobyl–vanadyl phosphates reveal an intermediate behavior in com-

(19) Bordes, E.; Courtine, P. *J. Catal.* 1979, 57, 236–252.

(20) Pulvin, S.; Bordes, E.; Ronis, M.; Courtine, P. *J. Chem. Res., Miniprint* 1981, 362–373.

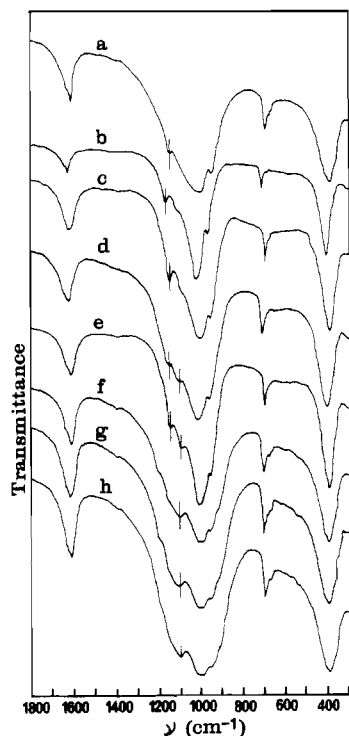


Figure 6. Infrared spectra of (a) $\text{NbOPO}_4 \cdot 3\text{H}_2\text{O}$, (b) $(\text{V}_{0.04}\text{Nb}_{0.96})\text{OPO}_4 \cdot 2.7\text{H}_2\text{O}$, (c) $(\text{V}_{0.06}\text{Nb}_{0.94})\text{OPO}_4 \cdot 2.7\text{H}_2\text{O}$, (d) $(\text{V}_{0.10}\text{Nb}_{0.90})\text{OPO}_4 \cdot 2.8\text{H}_2\text{O}$, (e) $(\text{V}_{0.11}\text{Nb}_{0.89})\text{OPO}_4 \cdot 2.8\text{H}_2\text{O}$, (f) $(\text{V}_{0.17}\text{Nb}_{0.83})\text{OPO}_4 \cdot 2.6\text{H}_2\text{O}$, (g) $(\text{V}_{0.21}\text{Nb}_{0.79})\text{OPO}_4 \cdot 2.8\text{H}_2\text{O}$, and (h) $(\text{V}_{0.21}\text{Nb}_{0.79})\text{OPO}_4 \cdot 2.7\text{H}_2\text{O}$.

parison with those of the pure precursors. Thus, while niobyl phosphate only shows an absorption band at 235 nm, in the vanadyl phosphate spectra, there are two wider bands that are centered at 290 and 420 nm due to charge transfer of the type $\text{L} \rightarrow \text{M}$ because they are metals in a high oxidation state (V) and with a $[\text{d}^0]$ configuration.

In the mixed-phosphate spectra, two bands appear at 240 and 335 nm; these are accompanied by a shoulder at 400 nm also assigned to charge transfer. It must be pointed out that the band at 290 nm in the vanadyl phosphate spectra appears to be displaced to 335 nm in the mixed phosphates. In Figure 7 it can be seen how, in the phosphates with the higher vanadium content, the intensity of the band at 240 nm decreases in comparison with that at 335 nm. On the other hand, the reduction of $\text{V(V)} \rightarrow \text{V(IV)}$ with CsI (Figure 8) provoked a drastic decrease in the intensity of the band at 335 nm to give rise to the appearance of d-d transitions in the visible region that correspond to $\text{V(IV)} [\text{d}^1]$, while the band at 240 nm does not vary. This confirms the assignment of the absorption band at 335 nm as that of the $\text{L} \rightarrow \text{V}$ charge transfer.

Conclusions

1. From solutions containing different $\text{V}/(\text{V} + \text{Nb})$ percentage molar ratios, mixed niobyl-vanadyl phosphates with different percentages of vanadium have been isolated. The maximum possible value of vanadium was 21%.

2. The hydrolysis of the mixed phosphates was more affected by temperature than the redox reactions $\text{V(V)} \rightarrow \text{V(IV)}$. At 50 °C the hydrolysis of mixed phosphates varied from 1.3 to 4.0% as the percentages of vanadium increased, while vanadyl phosphate was completely dissolved. However, the hydrolysis of the mixed phosphates caused by reduction of vanadium at 25 °C varied little: for the whole series the range was 0.2–1.0%. Under the same conditions vanadyl phosphate underwent a significant degree of hydrolysis (20%).

3. All mixed phosphates are indexable in the tetragonal system, with $a = b = 6.42\text{--}6.45 \text{ \AA}$ and $c = 15.76\text{--}15.98 \text{ \AA}$. The analysis

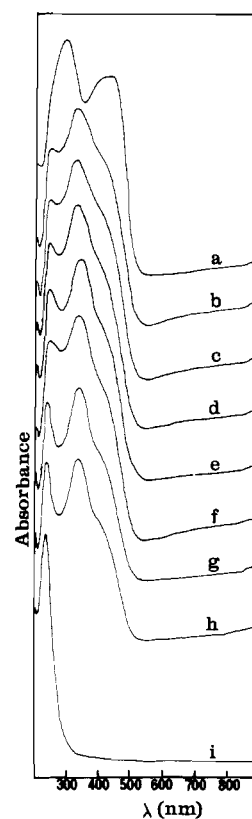


Figure 7. Diffuse-reflectance spectra of (a) $\text{VOPO}_4 \cdot 2\text{H}_2\text{O}$, (b) $(\text{V}_{0.21}\text{Nb}_{0.79})\text{OPO}_4 \cdot 2.7\text{H}_2\text{O}$, (c) $(\text{V}_{0.21}\text{Nb}_{0.79})\text{OPO}_4 \cdot 2.8\text{H}_2\text{O}$, (d) $(\text{V}_{0.17}\text{Nb}_{0.83})\text{OPO}_4 \cdot 2.6\text{H}_2\text{O}$, (e) $(\text{V}_{0.11}\text{Nb}_{0.89})\text{OPO}_4 \cdot 2.8\text{H}_2\text{O}$, (f) $(\text{V}_{0.10}\text{Nb}_{0.90})\text{OPO}_4 \cdot 2.8\text{H}_2\text{O}$, (g) $(\text{V}_{0.06}\text{Nb}_{0.94})\text{OPO}_4 \cdot 2.7\text{H}_2\text{O}$, (h) $(\text{V}_{0.04}\text{Nb}_{0.96})\text{OPO}_4 \cdot 2.7\text{H}_2\text{O}$, and (i) $\text{NbOPO}_4 \cdot 3\text{H}_2\text{O}$.

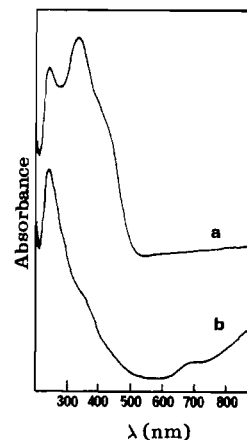


Figure 8. Diffuse-reflectance spectra of (a) $(\text{V}_{0.11}\text{Nb}_{0.89})\text{OPO}_4 \cdot 2.8\text{H}_2\text{O}$ and (b) the same compound after reduction with CsI.

of these compounds by EDX-SEM, DTA, IR spectra, X-ray diffraction and diffuse-reflectance spectra established that in every case the mixed phosphates were solid solutions of VOPO_4 in NbOPO_4 .

Acknowledgment. We thank the CICYT (Project No. PB86-0244) for financial support and Dr. Olivera Pastor for helpful discussions. We are grateful to David W. Schofield for reviewing the English version.

Registry No. $(\text{V}_{0.04}\text{Nb}_{0.96})\text{OPO}_4 \cdot n\text{H}_2\text{O}$, 115561-96-1; $(\text{V}_{0.06}\text{Nb}_{0.94})\text{OPO}_4 \cdot n\text{H}_2\text{O}$, 115561-98-3; $(\text{V}_{0.10}\text{Nb}_{0.90})\text{OPO}_4$, 115603-39-9; $(\text{V}_{0.11}\text{Nb}_{0.89})\text{OPO}_4 \cdot n\text{H}_2\text{O}$, 115590-73-3; $(\text{V}_{0.17}\text{Nb}_{0.83})\text{OPO}_4 \cdot n\text{H}_2\text{O}$, 115562-00-0; $(\text{V}_{0.21}\text{Nb}_{0.79})\text{OPO}_4 \cdot n\text{H}_2\text{O}$, 115562-02-2; $\text{NbOPO}_4 \cdot 3\text{H}_2\text{O}$, 106762-97-4; $\text{VOPO}_4 \cdot 2\text{H}_2\text{O}$, 12293-87-7.